594–599 *Nucleic Acids Research, 2012, Vol. 40, No. 2* *Published online 19 September 2011*
doi:10.1093/nar/gkr760

RDR6-mediated synthesis of complementary RNA is terminated by miRNA stably bound to template RNA

Rajendran Rajeswaran and Mikhail M. Pooggin*

Institute of Botany, University of Basel, Schönbeinstrasse 6, 4056 Basel, Switzerland

Received August 3, 2011; Revised August 24, 2011; Accepted August 30, 2011

ABSTRACT

RNA-dependent RNA polymerase RDR6 is involved in the biogenesis of plant *trans*-acting siRNAs. This process is initiated by miRNA-directed and Argonaute (AGO) protein-mediated cleavage of *TAS* gene transcripts. One of the cleavage products is converted by RDR6 to double-stranded (ds)RNA, the substrate for Dicer-like 4 (DCL4). Interestingly, *TAS3* transcript contains two target sites for miR390::AGO7 complexes, 5′-non-cleavable and 3′-cleavable. Here we show that RDR6-mediated synthesis of complementary RNA starts at a third nucleotide of the cleaved *TAS3* transcript and is terminated by the miR390::AGO7 complex stably bound to the non-cleavable site. Thus, the resulting dsRNA has a short, 2-nt, 3′-overhang and a long, 220-nt, 5′-overhang of the template strand. The short, but not long, overhang is optimal for DCL4 binding, which ensures dsRNA processing from one end into phased siRNA duplexes with 2-nt 3′-overhangs.

INTRODUCTION

The biogenesis of plant *trans*-acting short interfering (si) RNAs (tasiRNAs) is initiated by microRNA (miRNA)-directed and Argonaute (AGO) protein-mediated cleavage of a primary RNA (pri-RNA) transcribed by Pol II from a *TAS* gene. One of the pri-RNA cleavage products is fully or partially converted by RNA-dependent RNA polymerase (RDR) 6 (RDR6) to double-stranded RNA (dsRNA). The dsRNA is processed by Dicer-like 4 (DCL4) from the miRNA cleavage terminus into several consecutive 21-nt siRNA duplexes with 2-nt 3′-overhangs (1,2). One of the duplex strands (mature tasiRNA) binds an AGO protein and guides the resulting RNA-induced silencing complex (RISC) to complementary target mRNAs. The RISC complex interaction with target mRNA leads to its silencing through AGO-mediated cleavage or translational repression.

In *Arabidopsis thaliana*, three miRNAs are known to initiate tasiRNA biogenesis: miR173, miR390 and miR828 (1,3). The miR173-dependent tasiRNAs are encoded in *TAS1a/b/c* and *TAS2* genes and target several genes of the pentatricopeptide repeat gene family and those of unknown function. The miR828-dependent tasiRNA is encoded in *TAS4* and targets three members of MYB (myeloblastosis) transcription factor gene family. The miR390-dependent tasiRNAs, also called tasiARFs, are encoded in three *TAS3* family genes (*3a*, *3b* and *3c*) and target the genes from auxin response factor (*ARF*) family including *ARF3/ETTIN* and *ARF4* that regulate plant development. Only *TAS3*-derived tasiARF species are conserved in higher plants. Here we used *TAS3a*, the most highly expressed *TAS3* family gene (4), to address some of the unknowns of tasiRNA biogenesis and, specifically, to determine the structures of RDR6-dependent dsRNA precursors of tasiARFs.

To guide cleavage of *TAS3a/b/c* pri-RNAs and thereby initiate tasiARF biogenesis, miR390 binds AGO7 to form a miR390–AGO7 complex with slicer activity (5). Importantly, all the three *TAS3* pri-RNAs carry a second, non-cleavable, miR390 complementary site, 190–230 nt upstream of the miR390 cleavage site (4) (Figure 1A). The non-cleavable interaction of the miR390–AGO7 complex with *TAS3a* pri-RNA is absolutely necessary for RDR6-dependent tasiARF production: the non-cleavable site sequence could neither tolerate mutations that destabilize the complementary interaction, nor be functionally substituted by unrelated target sequences fully or partially complementary to a heterologous miRNA, e.g. AGO1-associated miR171a (5,6). In contrast, the miR390 cleavage site sequence could be functionally replaced with the miR171 cleavage site sequence (5). The specific function of the miR390–AGO7 complex at the non-cleavable site is not known. It has been proposed that a stable interaction of this complex with cleaved *TAS3* pri-RNAs passively or actively recruits RDR6 to the cleaved pri-RNA 3′-terminus, where complementary RNA synthesis is to be initiated (5). The fact that the region of all the three *TAS3* genes between the two target sites spawns the majority of RDR6-dependent siRNAs including tasiARFs (4) led us to propose that RDR6 synthesis of complementary RNA

*To whom correspondence should be addressed. Tel: +4161 2672977; Fax +4161 2673504; Email: Mikhail.Pooggin@unibas.ch

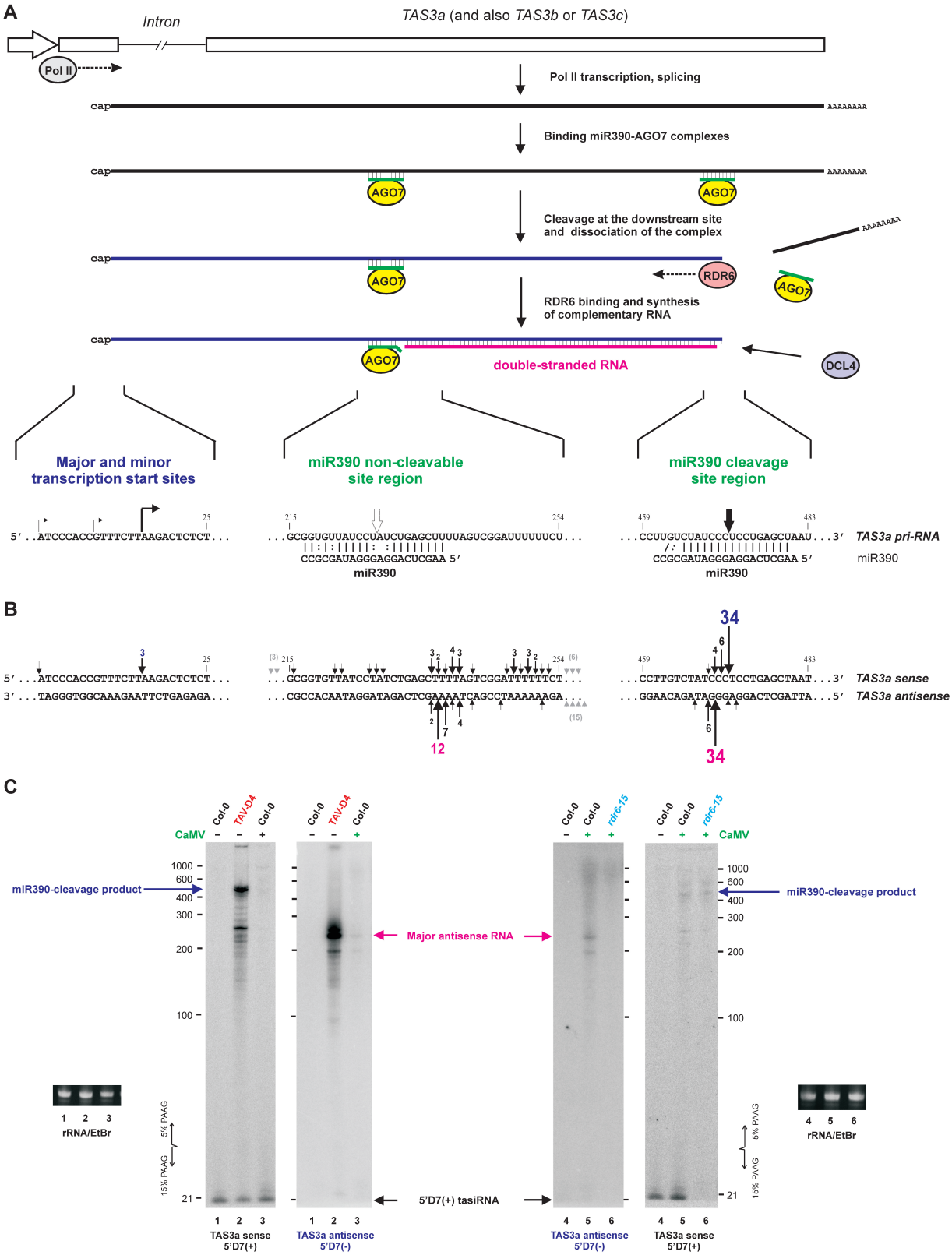

Figure 1. Model for the biogenesis of a dsRNA precursor of *TAS3a* tasiRNA and cRT–PCR sequencing of the dsRNA termini. (**A**) Diagrammatic representation of *TAS3* dsRNA biogenesis. *TAS3a* gene is transcribed by Pol II into a capped and polyadenylated pri-RNA, followed by splicing. The spliced pri-RNA is associated with two miR390–AGO7 complexes at the respective upstream (non-cleavable) and downstream (cleavable) target sites. The downstream complex cleaves pri-RNA and dissociates from the 5′-cleavage product, the template for RDR6. RDR6 is recruited to the 3′-end of the template and initiates complementary RNA synthesis. The upstream miR390–AGO7 complex stably bound to the template terminates RDR6 synthesis. The sequences surrounding the *TAS3a* transcription start and miR390 target sites are shown in the expanded regions. The major

(continued)

is terminated by the miR390–AGO7 complex stably bound to the template RNA. Here, we tested this hypothesis by sequencing of RDR6-synthesized complementary RNA derived from *TAS3a* gene.

MATERIALS AND METHODS

Seedlings of *Arabidopsis* wild-type (Col-0 and La-er) and mutant lines *dcl2/3/4* (7), *zip-2* [*ago7*; (8,9)] and *rdr6-15* (1) were grown and infected with Cauliflower mosaic virus (CaMV) as described previously (7). The *Arabidopsis* transactivator/viroplasmin (TAV) transgenic line D4-2 was generated and characterized earlier (10,11). Our previously described protocols were used for total RNA preparation (12), high resolution blot hybridization (11) and circularization-reverse transcription–PCR (cRT–PCR) [(13,14); also see 'Protocol' in Supplementary Data]. The hybridization probes and cRT–PCR primers are listed in Supplementary Table S1.

RESULTS AND DISCUSSION

Under normal conditions, dsRNA precursors of tasiRNAs are rapidly processed by DCL4 and therefore, accumulate to the levels barely detectable by RNA blot hybridization. To characterize the structures of *TAS3a*-derived dsRNA(s) we made use of *Arabidopsis* Col-0 and La-er plants infected with CaMV or transgenic Col-0 plants expressing a CaMV TAV protein. Both CaMV infection and TAV expression stabilize dsRNAs derived from *TAS1a/b/c*, *TAS2* and *TAS3a* genes (11). In the case of *TAS3a*, transgene expression of TAV derived from CaMV strain D4 (TAV-D4) had the strongest stabilization effect (11). Here, we performed a higher resolution blot hybridization analysis of *TAS3a*-derived long sense and antisense RNAs using DNA oligonucleotide probes specific for *TAS3a* siRNAs 5′D7(+) and 5′D7(−), i.e. sense and antisense strands of the 5′D7 duplex located between the two miR390 target sites. In sense polarity, a very abundant RNA of ~460 nt and several shorter, less abundant RNAs ranging from 140 nt to 330 nt accumulated in TAV-D4 plants. These RNAs accumulated at much lower levels in CaMV-infected Col-0 plants (Figure 1C). The estimated size of the most abundant sense RNA corresponds to that of the 5′-cleavage product of *TAS3a* pri-RNA mapped previously by 5′- and 3′-RACE (4) (rapid amplification of complementary DNA ends) (Figure 1A).

In antisense polarity, a very abundant RNA of ~230 nt and less abundant, shorter (~200 nt) and longer (~250 nt) RNAs accumulated in TAV-D4 plants (Figure 1C). The 230-nt and 200-nt RNAs were also detected in Col-0 and La-er plants, albeit at much lower levels. Genetic evidence revealed that both of these antisense RNAs are RDR6-dependent, unlike the 460-nt sense RNA, they did not accumulate in *rdr6-15* null mutant plants (Figure 1C). The 230-nt (but not 200-nt) antisense RNA accumulated in triple null mutant plants lacking DCL2, DCL3 and DCL4 activities [*dcl2/3/4* in Col-0 background; (7)] (Supplementary Figure S1A). This indicates that the 230-nt RNA is a complete RDR6 transcript and hence the complementary strand of *TAS3a*-derived major dsRNA. The 200-nt RNA may represent a complementary strand of a shorter dsRNA produced via a secondary, *in cis* cleavage of *TAS3a* pri-RNA by TAS3a siRNA 5′D2(−) which was reported previously (1). Both antisense RNAs did not accumulate in *AGO7* null mutant plants (Supplementary Figure S1A), thus confirming an essential role of AGO7 in the biogenesis of dsRNA precursors of tasiARFs. Taken together, our results suggest that the major dsRNA derived from *TAS3a* gene is an asymmetrical duplex composed of ~450-nt sense RNA (miR390-cleavage product of *TAS3a* pri-RNA) and ~230-nt antisense RNA (RDR6 transcript).

To precisely map the RDR6 transcript, we used a cRT–PCR method that enables simultaneous cloning and sequencing of both 5′- and 3′-terminal regions of a given RNA [(13); schematically shown in Supplementary Figure S1B]. Since RDR6 activity does not require a primer (15), the 5′-terminal nucleotide of an RDR6 transcript is likely 5′-triphosphorylated. To circularize such a transcript, prior to RNA ligation, total plant RNA was treated with pyrophosphatase which converts a 5′-polyphosphorylated or capped nucleotide to a 5′-monophosphorylated nucleotide. The cRT–PCR primers proximal to the termini of *TAS3a*-derived major antisense RNA were designed based on the size estimated by blot hybridization (Figure 1C). The major cRT–PCR products of expected size obtained from TAV-D4 transgenic and CaMV-infected *dcl2/3/4* plant samples were gel-purified, cloned and individual clones were sequenced.

For both samples, cRT–PCR analysis (Supplementary Figure S1C; summarized in Figure 1B) revealed that

Figure 1. Continued
and minor transcription start sites mapped previously [by Howell *et al.* (4)] are indicated by the big and small broken arrows, respectively. The numbering is from the 5′-end of the longest cDNA representing *TAS3a* pri-RNA. The miR390 basepairing to the non-cleavable and cleavable sites are shown and position of the expected cleavage is indicated with open or filled arrows, respectively. (**B**) cRT–PCR mapping of the *TAS3a* sense and antisense RNAs (Supplementary Figure S1C for details). Sequences of *TAS3a* gene surrounding the transcription start and two miR390 target sites are shown in sense and antisense orientation. The numbering is as in (A). The termini of sequenced cRT–PCR clones are indicated by arrows above the sequence for sense RNAs (a total of 45 clones) and below the sequence for antisense RNAs (a total of 44 clones). The number of clones is given when more than one clone had the same 5′- or 3′-terminus. Additional clones that map outside of the shown sequences are indicated by grey arrows with a total number of the clones given in brackets above the sense strand and below the antisense strand. (**C**) RNA blot hybridization analysis of *TAS3a* sense and antisense RNAs accumulating in CaMV-infected (+) or mock inoculated (−) wild-type (Col-0) and *rdr6* mutant (*rdr6-15*) plants or plants transgenic for CaMV TAV protein (TAV-D4). The polyacrylamide gel (PAAG) was composed of 5% upper part and 15% lower part as indicated. Two blots shown on the left and on the right were hybridized successively with probes specific to sense and antisense strands of the TAS3a 5′D7 siRNA duplex. The 21-nt guide stand of this duplex accumulates in wild-type but not *rdr6* mutant plants (indicated by arrow). Positions of single-stranded RNA markers ranging from 100 nt to 1000 nt are indicated. The 5′-cleavage product of *TAS3a* pri-RNA and the major antisense RNA (RDR6 product) are indicated by blue and magenta arrows, respectively. rRNA stained with EtBr is shown as loading control.

the major antisense RNA begins predominantly with G469 [the numbering is from a 5′-terminal nucleotide of the longest cDNA representing a spliced *TAS3a* pri-RNA (4); Figure 1A]: 34 of 44 clones mapped to this position, while only 6 clones mapped to A468. Hence, RDR6 initiates complementary RNA synthesis predominantly at the third nucleotide from the 3′-terminus of the miR390–AGO7-cleaved *TAS3a* pri-RNA. This creates a 2-nt 3′-overhang on the resulting dsRNA. A similar property was reported for an RDR activity isolated from tomato plants: *in vitro*, it initiated synthesis of complementary RNA at either the second or the third nucleotide from artificial RNA template's 3′-hydroxylated terminus (16).

The 3′-termini of cloned antisense RNAs were more heterogeneous, but 29 of 44 clones clustered in a close vicinity of the miR390 non-cleavable target site. This location fits the estimated size of the major antisense RNA detected by blot hybridization. Two major fractions of the antisense RNA terminate with A237 (12 clones) and A238 (7 clones), while two minor fractions terminate with A236 (2 clones) and U240 (4 clones) (Figure 1B). Thus, the predominant 3′-terminal nucleotide of the RDR6 transcript (A237) is complementary to the last nucleotide of the miR390 non-cleavable target sequence, which can potentially pair with the 5′-terminal nucleotide of miR390 (Figure 1A). Based on crystal structures of *Thermus thermophilus* AGO-guide strand complexes (17), it can be envisaged that the 5′-phosphate of miR390 is sequestered in the binding pocket of AGO7 protein and therefore, the 5′-terminal nucleotide cannot pair with the complementary nucleotide of the target site. Hence, this complementary nucleotide can potentially be copied by RDR6 without displacement of the miR390/template RNA complex. Only a minor fraction of the RDR6 transcript terminates at A236, pairing with the second nucleotide of miR390, whereas, the second largest fraction terminates just in front of the target site (A238). We conclude that RDR6-mediated synthesis of complementary RNA is effectively terminated by the miR390–AGO7 complex stably bound to the target site (Figure 1A). RDR6 appears to be unable to displace this complex and proceed with synthesis of complementary RNA further upstream, towards the template's 5′-end.

We next used cRT–PCR with reverse primers in order to precisely map *TAS3a* sense RNAs. The design of cRT–PCR with the RT primer located about 40 nt downstream of the miR390 non-cleavable site (Supplementary Figure S1C) allowed us not only to pick up the previously mapped, 5′-cleavage product of pri-RNA (the most abundant RNA of ~450 nt, stabilized by CaMV TAV) but also to analyze less abundant, shorter RNAs in the size range starting from ~200 nt. Note that this design was biased towards the shorter RNAs, despite their lower abundance. Confirming the previous 5′-RACE mapping results (4), our analysis (Supplementary Figure S1C; summarized in Figure 1B) revealed that the 5′-cleavage product of *TAS3a* pri-RNA, i.e. the presumptive template for RDR6, starts predominantly at A16, i.e. at the major transcription start site located 16 nt downstream of the most distal, minor transcription start site (Figure 1A). Both, the 5′-cleavage product and shorter *TAS3a* sense RNAs terminate predominantly at C471 (34 of 45 clones), which corresponds to the miR390-directed cleavage between nucleotides 10 and 11 from the miR390 5′-end (Figure 1A). A small fraction of sense RNA terminated at either T468 (1 clone), or C469 (4 clones), or C470 (6 clones) (Figure 1B and Supplementary Figure S1C). The RNA terminating with C470 could be a template for the minor fraction of RDR6 transcript starting with A468 which is complementary to the third nucleotide from this template's end.

Analysis of the *TAS3a*-derived shorter sense RNAs revealed that a large fraction of their 5′-termini fall heterogeneously in two clusters just downstream of the miR390 non-cleavable target site and a smaller fraction of the 5′-termini fall within or upstream of the target site sequence (Figure 1B and Supplementary Figure S1C). These results are consistent with the previous 5′-RACE mapping (4) showing no evidence for a precise, miR390-directed cleavage at this target site. Together with blot hybridization, cRT–PCR data also indicate that a fraction of the 5′-cleavage product of *TAS3a* pri-RNA is gradually truncated from the 5′-end before or after RDR6-mediated production of the asymmetrical dsRNA. A regular ladder of the truncated antisense RNAs (Figure 1C) points at involvement of a non-randomly terminating 5′–3′-exonuclease.

Taken together, our genetic analysis, RNA blot hybridization and cRT–PCR data suggest the following model for the biogenesis of dsRNA precursor of *TAS3a* tasiRNAs (Figure 1A): Two AGO7–miR390 complexes bind *TAS3a* pri-RNA at the upstream (non-cleavable) and downstream (cleavable) target sites and the downstream complex cleaves the target sequence between nucleotides 10 and 11 from the miR390 5′-end, followed by dissociation of this complex. The 5′-cleavage product of pri-RNA associated with the upstream complex serves as a template for RDR6. RDR6-mediated synthesis of complementary RNA is initiated at the third nucleotide from the template's 3′-end and terminated just in front of the miR390–AGO7 complex bound at the non-cleavable site. In most cases, the last nucleotide incorporated into the RDR6 transcript is complementary either to the template nucleotide located just downstream to the target sequence or to the last nucleotide of the target sequence. Only a minor fraction of RDR6 transcript is terminated one nucleotide further downstream, which would require partially melting the miR390/template RNA duplex. Thus, RDR6 appears to be unable to displace the miR390–AGO7 complex from the non-cleavable target site. The resulting dsRNA precursor of tasiARFs has an asymmetrical structure with two overhangs of the sense (template) strand: the long, 220-nt 5′-overhang and the short, 2-nt 3′-overhang (Figure 1A).

Interestingly, RNA duplexes with long 5′-overhangs are preferential *in vitro* binding substrates for SGS3 (18), the protein essential for tasiRNA biogenesis. The role of SGS3 in tasiRNA biogenesis is not known yet, although genetic evidence suggested that it stabilizes miRNA-cleaved pri-RNA (2).

Only the 2-nt 3′-overhang but not the long 5′-overhang is compatible with DCL4 binding and in-phase

processing of the asymmetric *TAS3a* dsRNA. Indeed, tasiARFs are encoded in the phase register set by miR390-directed cleavage. A 2-nt 3′-overhang is optimal for binding and processing miRNA precursors by recombinant human Dicer *in vitro* (19). Furthermore, the 2-nt 3′-overhang fits into the PAZ (Piwi/Argonaute/Zwille) domain binding pocket of *Giardia* Dicer (20). Four *Arabidopsis* DCLs including DCL4 possess a conserved PAZ domain (21,22) that might be involved in recognition of dsRNA substrates with 2-nt 3′-overhangs. Our parallel study of dsRNA precursors of *TAS1a*/*b*/*c*- and *TAS2*-derived tasiRNAs revealed that these dsRNAs have 1- or 2-nt 3′-overhangs which make them compatible with DCL4 processing from both ends (R. Rajeswaran *et al*., submitted for publication). In the case of *TAS3a*, and presumably *TAS3b* and *TAS3c*, both the long 5′-overhang of dsRNA precursor and the miR390–AGO7 complex that may remain associated with this overhang would prevent DCL4 binding, thus ensuring the correct processing of phased tasiRNAs only from the opposite terminus.

Stable association of miR390 with its non-cleavable target site on *TAS3* pri-RNA is further supported by a 'target mimicry' phenomenon, in which miR399 is effectively sequestered from cleavage-mediated silencing of its target mRNA by stable interaction with a non-cleavable, decoy target RNA (23). Notably, in both cases the pairing of a miRNA and a target RNA is interrupted by a mismatched loop at the expected miRNA cleavage site.

We demonstrate here that a non-cleavable interaction of miR390 and *TAS3a* pri-RNA terminates RDR6 synthesis and thereby, protects the sequences upstream of the miR390 binding site from being converted to dsRNA. This precludes production of additional siRNAs from the upstream region, which may potentially cause negative effects. The phenomenon of transitivity or spread of secondary siRNA production along miRNA/siRNA target genes has been described in plants (24) and *Caenorhabditis elegans* (25). In multigene families containing a miRNA target gene the transitivity can potentially lead to production of secondary siRNAs from the conserved region(s) with high nucleotide sequence similarity and therefore result in off-target cleavage and silencing of all the family members. In this case, a second, non-cleavable target site for miRNA/siRNA, which is located upstream of the cleavage site, would confine RDR-dependent siRNA production just to the short intervening region. This represents an additional function of the two-hit trigger mechanism of tasiRNA biogenesis proposed for *TAS3* family genes and other genes spawning RDR6-dependent siRNAs (4,6).

SUPPLEMENTARY DATA

Supplementary Data are available at NAR Online.

ACKNOWLEDGEMENTS

We thank Nachelli Malpica and Ekaterina Gubaeva for excellent technical assistance and Hailing Jin for *zip-2* seed. We are grateful to Thomas Hohn for his constant support and stimulating discussions and to Thomas Boller, Andres Wiemken and Christian Körner for hosting the group at the Botanical Institute. M.M.P. conceived and designed the experiments; R.R. performed the experiments; M.M.P. wrote the article.

FUNDING

The Swiss National Science Foundation (31003A_127514 to M.M.P.); the European Commission Marie Curie fellowship (PIIF-237493-SUPRA to R.R.). Funding for open access charge: University of Basel.

Conflict of interest statement. None declared.

REFERENCES

1. Allen,E., Xie,Z., Gustafson,A.M. and Carrington,J.C. (2005) microRNA-directed phasing during trans-acting siRNA biogenesis in plants. *Cell*, **121**, 207–221.
2. Yoshikawa,M., Peragine,A., Park,M.Y. and Poethig,R.S. (2005) A pathway for the biogenesis of trans-acting siRNAs in Arabidopsis. *Genes Dev*., **19**, 2164–2175.
3. Rajagopalan,R., Vaucheret,H., Trejo,J. and Bartel,D.P. (2006) A diverse and evolutionarily fluid set of microRNAs in Arabidopsis thaliana. *Genes Dev*., **20**, 3407–3425.
4. Howell,M.D., Fahlgren,N., Chapman,E.J., Cumbie,J.S., Sullivan,C.M., Givan,S.A., Kasschau,K.D. and Carrington,J.C. (2007) Genome-wide analysis of the RNA-dependent RNA polymerase6/dicer-like4 pathway in Arabidopsis reveals dependency on miRNA- and tasiRNA-directed targeting. *Plant Cell*, **19**, 926–942.
5. Montgomery,T.A., Howell,M.D., Cuperus,J.T., Li,D., Hansen,J.E., Alexander,A.L., Chapman,E.J., Fahlgren,N., Allen,E. and Carrington,J.C. (2008) Specificity of ARGONAUTE7-miR390 interaction and dual functionality in TAS3 trans-acting siRNA formation. *Cell*, **133**, 128–141.
6. Axtell,M.J., Jan,C., Rajagopalan,R. and Bartel,D.P. (2006) A two-hit trigger for siRNA biogenesis in plants. *Cell*, **127**, 565–577.
7. Blevins,T., Rajeswaran,R., Shivaprasad,P.V., Beknazariants,D., Si-Ammour,A., Park,H.S., Vazquez,F., Robertson,D., Meins,F. Jr, Hohn,T. *et al*. (2006) Four plant Dicers mediate viral small RNA biogenesis and DNA virus induced silencing. *Nucleic Acids Res*., **34**, 6233–6246.
8. Hunter,C., Sun,H. and Poethig,R.S. (2003) The Arabidopsis heterochronic gene ZIPPY is an ARGONAUTE family member. *Curr. Biol*., **13**, 1734–1739.
9. Katiyar-Agarwal,S., Gao,S., Vivian-Smith,A. and Jin,H. (2007) A novel class of bacteria-induced small RNAs in Arabidopsis. *Genes Dev*., **21**, 3123–3134.
10. Yu,W., Murfett,J. and Schoelz,J.E. (2003) Differential induction of symptoms in Arabidopsis by P6 of Cauliflower mosaic virus. *Mol. Plant Microbe. Interact*., **16**, 35–42.
11. Shivaprasad,P.V., Rajeswaran,R., Blevins,T., Schoelz,J., Meins,F. Jr, Hohn,T. and Pooggin,M.M. (2008) The CaMV transactivator/viroplasmin interferes with RDR6-dependent trans-acting and secondary siRNA pathways in Arabidopsis. *Nucleic Acids Res*., **36**, 5896–5909.
12. Akbergenov,R., Si-Ammour,A., Blevins,T., Amin,I., Kutter,C., Vanderschuren,H., Zhang,P., Gruissem,W., Meins,F. Jr, Hohn,T. *et al*. (2006) Molecular characterization of geminivirus-derived small RNAs in different plant species. *Nucleic Acids Res*., **34**, 462–471.
13. Shivaprasad,P.V., Akbergenov,R., Trinks,D., Rajeswaran,R., Veluthambi,K., Hohn,T. and Pooggin,M.M. (2005) Promoters, transcripts, and regulatory proteins of Mungbean yellow mosaic geminivirus. *J. Virol*., **79**, 8149–8163.
14. Blevins,T., Rajeswaran,R., Aregger,M., Borah,B.K., Schepetilnikov,M., Baerlocher,L., Farinelli,L., Meins,F., Hohn,T.

and Pooggin,M.M. (2011) Massive production of small RNAs from a non-coding region of Cauliflower mosaic virus in plant defense and viral counter-defense. *Nucleic Acids Res.*, **39**, 5003–5014.
15. Curaba,J. and Chen,X. (2008) Biochemical activities of Arabidopsis RNA-dependent RNA polymerase 6. *J. Biol. Chem.*, **283**, 3059–3066.
16. Schiebel,W., Haas,B., Marinković,S., Klanner,A. and Sänger,H.L. (1993) RNA-directed RNA polymerase from tomato leaves. II. Catalytic in vitro properties. *J. Biol. Chem.*, **268**, 11858–11867.
17. Wang,Y., Juranek,S., Li,H., Sheng,G., Wardle,G.S., Tuschl,T. and Patel,D.J. (2009) Nucleation, propagation and cleavage of target RNAs in Ago silencing complexes. *Nature*, **461**, 754–761.
18. Fukunaga,R. and Doudna,J.A. (2009) dsRNA with 5′ overhangs contributes to endogenous and antiviral RNA silencing pathways in plants. *EMBO J.*, **28**, 545–555.
19. Zhang,H., Kolb,F.A., Jaskiewicz,L., Westhof,E. and Filipowicz,W. (2004) Single processing center models for human Dicer and bacterial RNase III. *Cell*, **118**, 57–68.
20. Macrae,I.J., Zhou,K., Li,F., Repic,A., Brooks,A.N., Cande,W.Z., Adams,P.D. and Doudna,J.A. (2006) Structural basis for double-stranded RNA processing by Dicer. *Science*, **311**, 195–198.
21. Schauer,S.E., Jacobsen,S.E., Meinke,D.W. and Ray,A. (2002) DICER-LIKE1: blind men and elephants in Arabidopsis development. *Trends Plant Sci.*, **7**, 487–491.
22. Dunoyer,P., Himber,C. and Voinnet,O. (2005) DICER-LIKE 4 is required for RNA interference and produces the 21-nucleotide small interfering RNA component of the plant cell-to-cell silencing signal. *Nat. Genet.*, **37**, 1356–1360.
23. Franco-Zorrilla,J.M., Valli,A., Todesco,M., Mateos,I., Puga,M.I., Rubio-Somoza,I., Leyva,A., Weigel,D., García,J.A. and Paz-Ares,J. (2007) Target mimicry provides a new mechanism for regulation of microRNA activity. *Nat. Genet.*, **39**, 1033–1037.
24. Himber,C., Dunoyer,P., Moissiard,G., Ritzenthaler,C. and Voinnet,O. (2003) Transitivity-dependent and -independent cell-to-cell movement of RNA silencing. *EMBO J.*, **22**, 4523–4533.
25. Sijen,T., Fleenor,J., Simmer,F., Thijssen,K.L., Parrish,S., Timmons,L., Plasterk,R.H. and Fire,A. (2001) On the role of RNA amplification in dsRNA-triggered gene silencing. *Cell*, **107**, 465–476.